AIAA JOURNAL
Vol. 33, No. 9, September 1995

Fourier Solution to Higher Order Theory Based Laminated Shell Boundary-Value Problem

Reaz A. Chaudhuri*
University of Utah, Salt Lake City, Utah 84112
and
Humayun R. H. Kabir†
University of Kuwait, Safat 13060, Kuwait

A complete (i.e., particular as well as complementary) Fourier solution to the boundary-value problem of static response under transverse load of a general cross-ply thick doubly curved panel of rectangular planform is presented. A boundary-discontinuous double Fourier series approach is used to solve a system of five partial differential equations, generated by a higher order shear deformation theory-based shell analysis, with the SS2-type of simply supported boundary condition prescribed at all four edges. Unlike the conventional Navier and Levy type approaches which can only provide particular solutions, the present method is general enough to provide the complete (particular as well as the complementary) solution for any arbitrary combination of admissible boundary conditions with almost equal ease. The numerical accuracy of the solution is ascertained by studying the convergence characteristics of deflections and moments of cross-ply spherical panels and also by comparison with the available first-order shear deformation theory- and classical lamination theory-based analytical solutions. Hitherto unavailable important numerical results presented include sensitivity of the predicted response quantities of interest to lamination, boundary constraint, and thickness and curvature effects, as well as their interactions.

Introduction

RECENT years have witnessed an increasing use of advanced composite materials (e.g., graphite/epoxy, boron/epoxy, Kevlar®/epoxy, graphite/PEEK, etc.), which are replacing metallic alloys in the fabrication to flat/curved panels because of many beneficial properties, such as higher strength-to-weight ratios, longer fatigue (including sonic fatigue) life, better stealth characteristics, enhanced corrosion resistance, and most significantly the possibility of optimal design through the variation of stacking pattern, fiber orientation, and so forth, known as composite tailoring. Since the matrix material is of relatively low shearing stiffness as compared to the fibers, a reliable prediction of the response of these laminated shells must account for transverse shear deformation. Additionally, a solution to the problem of deformation of laminated shells and panels of finite dimensions must satisfy the prescribed boundary conditions, which introduce additional complexities into the analysis. The majority of the investigations on laminated shells and panels utilize either the classical lamination theory (CLT), which corresponds to the Love–Kirchhoff hypothesis (Love's first approximation theory) for homogeneous shells, or the first-order shear deformation theory (FSDT), based on the Mindlin[1] hypothesis. Superiority of the FSDT over the CLT in prediction of the transverse deflection of a moderately thick panel notwithstanding, the former theory requires incorporation of a shear correction factor, due to the fact that the FSDT assumes a uniform transverse shear strain distribution through the thickness, which violates equilibrium conditions at the top and bottom surfaces of the panel.

Noor and Burton[2,3] have presented extensive surveys on shear deformation theories and computational models relating to laminated shells. Exact three-dimensional elasticity solutions for rectangular cross-ply plates for a specific type of simply supported boundary condition are due to Pagano[4] and Srinivas and Rao.[5] Approximate thick plate/shell theories can be classified into two categories: 1) discrete layer approach[6–8] and 2) continuous inplane displacement through thickness. The former approach appears to be more suitable for numerical methods, such as the finite element methods (FEM). Additionally, postprocessing type methods used in conjunction with a discrete layer approach have yielded highly accurate interlaminar shear stress distribution through the thickness of symmetric and unsymmetric laminated plates and shells.[9–12]

Basset[13] appears to have been the first to suggest that the displacements can be expanded in power series of the thickness coordinate ξ_3. Following Basset's lead, second and higher order shear deformation theories (HSDT), involving continuous in-plane displacements through the thickness of thick laminated plates/shells, have been developed as special cases of the three-dimensional elasticity theory by Nelson and Lorch,[14] Murthy,[15] Levinson,[16] Reddy and Liu,[17] Librescu et al.[18] and many others to account for the aforementioned shear correction factor. An in-depth review of the literature reveals that although FSDT-based complete analytical or strong form of solutions for rectangular cross-ply plates and doubly curved panels have recently become available for general combinations of admissible boundary conditions (e.g., Chaudhuri and Kabir[19]), their HSDT-based counterparts still appear to be limited to the Navier- or Levy-type of solution, where a specific type of simply supported (i.e., SS3) boundary condition needs to be prescribed at either all four edges (Navier's method) or two opposite edges (Levy's approach). For example, Reddy and Liu[17] have presented an HSDT-based analysis for shallow cross-ply doubly curved panels of rectangular planform, with the SS3-type (designated by Hoff and Rehfield[20]) of simply supported boundary condition prescribed at all four edges. More recently, Librescu et al.[18] have obtained HSDT-based analytical solutions of shallow cross-ply doubly curved panels for various boundary conditions, following a Levy-type of approach, where two opposite edges are considered invariably simply supported (SS3 type). Approximate methods based on Ritz and Galerkin approaches that include among others the finite element methods yield weak (or integral) form of solutions. It is important to note that the strong (or differential) and weak forms of solutions are fundamentally different in that solutions are sought in different function spaces. For the problem under investigation, a strong form of solution will necessitate that the solution sought must belong to a space of square integrable functions with square integrable first and second derivatives in the interior of the domain, whereas for a weak form of solution the restriction of square inte-

Received Dec. 14, 1993; revision received Nov. 5, 1994; accepted for publication Nov. 29, 1994.

*Associate Professor, Department of Civil Engineering. Senior Member AIAA.

†Assistant Professor, Department of Civil Engineering, P.O. Box 5969.

grable second derivatives need not be imposed (see Hughes[21] for definition). Needless to say, the space of functions that meets the requirements of the strong form of solutions to the aforementioned boundary-value problems is severely restricted as compared to its weak counterpart, which explains the paucity of the strong form of solutions to this important class of plate/shell boundary-value problems. It is, therefore, a challenge to find this type of strong form of solutions also taking into account the completeness criterion, which is the primary objective of the present investigation.

In what follows, a hitherto unavailable HSDT-based complete boundary-discontinuous Fourier solution to the problem of general cross-ply doubly curved (albeit with constant curvatures) panels with the SS2 type simply supported boundary condition, prescribed at all four edges is derived. Unlike the Navier- and Levy-type of approaches, which can only provide particular solutions, the present method is general enough to provide the complete (particular as well as the complementary) solution for any arbitrary combination of admissible boundary conditions with almost equal ease. The numerical accuracy of the present solution is ascertained by studying its convergence characteristics and also by comparison with the available analytical solutions. Numerical results for various aspect and curvature ratios are presented to understand the complex deformation behavior of symmetric and antisymmetric cross-ply doubly curved panels. Since the corresponding complete CLT and FSDT results for the SS2 type boundary conditions are now available,[19] the present study investigates in depth the range of validity of these two theories, as applied to cross-ply shells, which is the final objective of this investigation.

Statement of the Problem

Figure 1 shows the geometry of a laminated shell of thickness h. An orthogonal curvilinear coordinate system is used to represent its geometry. Orthogonal curvilinear axes ξ_1 and ξ_2 are placed at the midsurface of the shell ($\xi_3 = 0$), and the ξ_3 coordinate is a straight line normal to the midsurface. The symbols a and b represent the curved span lengths of the two sides of the panel parallel to the ξ_1 and ξ_2 axes, respectively, whereas R_1 and R_2 denote the principal radii of the midsurface of the shell. Strain-displacement relations from the linear (small deformation) theory of elasticity in curvilinear coordinates are given as follows[22,23]:

$$\varepsilon_1(\xi_1,\xi_2,\xi_3) = \frac{1}{[1+(\xi_3/R_1)]g_1}\left[\bar{u}_{1,1} + \frac{1}{g_2}g_{1,2}\bar{u}_2 + \frac{g_1}{R_1}\bar{u}_3\right]$$

$$\varepsilon_3(\xi_3) = \bar{u}_{3,3} \tag{1}$$

$$\varepsilon_4(\xi_1,\xi_2,\xi_3) = \frac{1}{[1+(\xi_3/R_1)]g_1}\left[\bar{u}_{3,1} - \frac{g_1}{R_1}\bar{u}_1\right] + \bar{u}_{1,3}$$

$$\varepsilon_6(\xi_1,\xi_2,\xi_3) = \frac{1}{[1+(\xi_3/R_1)]g_1}\left(\bar{u}_{2,1} - \frac{1}{g_2}g_{1,2}\bar{u}_1\right) + \frac{1}{[1+(\xi_3/R_2)]g_2}\left(\bar{u}_{1,2} - \frac{1}{g_1}g_{2,1}\bar{u}_2\right)$$

where $\bar{u}_i (i = 1, 2, 3)$ and $\varepsilon_i (i = 1, \ldots, 6)$ represent the physical components of the displacement vector and strain tensor, respectively, at a point (ξ_1, ξ_2, ξ_3) on a parallel surface, whereas g_1 and g_2 are the first fundamental quantities of the shell reference surface

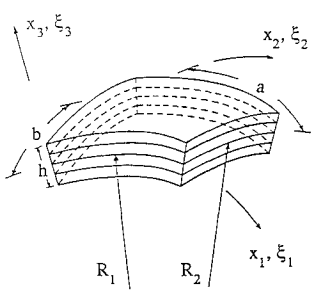

Fig. 1 Laminated doubly curved panel of rectangular planform.

for lines of curvature coordinates. Components ε_2 and ε_5 can be obtained from ε_1 and ε_4, respectively, by replacing subscript 1 by 2 and vice versa. To model the kinematic behavior of shells, an additional set of simplifying assumptions are invoked: 1) transverse inextensibility, 2) shallowness, and 3) negligibility of geodesic curvature. As mentioned earlier, the in-plane displacements can be expanded in power series of ξ_3, as suggested by Basset.[13] Retaining up to cubic terms and satisfying the conditions of transverse shear stresses (and hence strains) vanishing at a point $(\xi_1, \xi_2, \pm h/2)$ on the top and bottom surfaces of the shell yields[17]

$$\bar{u}_i = \left(1 + \frac{\xi_3}{R_i}\right)u_i + \xi_3\phi_i - \xi_3^3\frac{4}{3h^2}\left(\phi_i + \frac{1}{g_i}u_{3,i}\right) \qquad i = 1, 2 \text{ (no sum on } i) \tag{2}$$

$$\bar{u}_3 = u_3$$

where $\bar{u}_i (i = 1, 2, 3)$ are displacements of a point at the midsurface ($\xi_3 = 0$), whereas ϕ_1 and ϕ_2 are rotations about the ξ_2 and ξ_1 axes, respectively. Substitution of Eq. (2) into Eq. (1) supplies the following strain-displacement relations[17]:

$$\varepsilon_1 = \varepsilon_1^0 + \xi_3\left(\kappa_1^0 + \xi_3^2\kappa_1^2\right); \qquad \varepsilon_2 = \varepsilon_2^0 + \xi_3\left(\kappa_2^0 + \xi_3^2\kappa_2^2\right)$$

$$\varepsilon_4 = \varepsilon_4^0 + \xi_3^2\kappa_4^1; \qquad \varepsilon_5 = \varepsilon_5^0 + \xi_3^2\kappa_5^1$$

$$\varepsilon_6 = \varepsilon_6^0 + \xi_3\left(\kappa_6^0 + \xi_3^2\kappa_6^2\right) \tag{3}$$

where

$$\varepsilon_1^0 = u_{1,1} + \frac{u_3}{R_1}; \qquad \kappa_1^0 = \phi_{1,1}; \qquad \kappa_1^2 = -\frac{4}{3h^2}(\phi_{1,1} + u_{3,11})$$

$$\varepsilon_2^0 = u_{2,2} + \frac{u_3}{R_2}; \qquad \kappa_2^0 = \phi_{2,2}; \qquad \kappa_2^2 = -\frac{4}{3h^2}(\phi_{2,2} + u_{3,22})$$

$$\varepsilon_4^0 = \phi_2 + u_{3,2}; \qquad \kappa_4^1 = -\frac{4}{h^2}(\phi_2 + u_{3,2}); \qquad \varepsilon_5^0 = \phi_1 + u_{3,1}$$

$$\kappa_5^1 = -\frac{4}{h^2}(\phi_1 + u_{3,1}); \qquad \varepsilon_6^0 = u_{2,1} + u_{1,2}$$

$$\kappa_6^0 = \phi_{2,1} + \phi_{1,2}; \qquad \kappa_6^2 = -\frac{4}{3h^2}(\phi_{2,1} + \phi_{1,2} + 2u_{3,12}) \tag{4}$$

expressed in Cartesian curvilinear coordinate system ($dx_i = g_i d\xi_i$, no sum, $i = 1, 2$; and $\xi_3 = x_3$). The governing partial differential equations (PDEs) derived using the principle of virtual work[17] are

$$N_{1,1} + N_{6,2} = 0 \tag{5a}$$

$$N_{6,1} + N_{2,2} = 0 \tag{5b}$$

$$Q_{1,1} + Q_{2,2} - \frac{4}{h^2}(K_{1,1} + K_{2,2}) + \frac{4}{3h^2}(P_{1,11} + P_{2,22} + 2P_{6,12}) - \frac{N_1}{R_1} - \frac{N_2}{R_2} + q = 0 \tag{5c}$$

$$M_{1,1} + M_{6,2} - Q_1 + (4/h^2)K_1 - (4/h^2)(P_{1,1} + P_{6,2}) = 0 \tag{5d}$$

$$M_{6,1} + M_{2,2} - Q_2 + (4/h^2)K_2 - (4/h^2)(P_{6,1} + P_{2,2}) = 0 \tag{5e}$$

where q is the distributed transverse load, and N_i, M_i, and P_i ($i = 1, 2, 6$) denotes stress resultants, stress couples, and second stress couples (resultants of the second moment of stress) and are as defined by Reddy and Liu.[17] Q_i ($i = 4, 5$) represents the transverse shear stress resultants. The generalized stress resultants (i.e., stress resultants, stress couples, and second stress couples) can be conveniently expressed in terms of the strain components by utilizing the constitutive relations in the form of the generalized Hooke's law for orthotropic materials and integrating through the shell thickness.[17] Substitution of these generalized stress resultants into Eqs. (5) yields

a system of five highly coupled fourth-order PDE's. For example, the equilibrium equation (5c) yields

$$\begin{aligned} &G(3,\ 1)u_{1,\ 1} + G(3,\ 2)u_{1,\ 111} + G(3,\ 3)u_{1,\ 122} + G(3,\ 4)u_{2,\ 112} \\ &+ G(3,\ 5)u_{2,\ 2} + G(3,\ 6)u_{2,\ 222} + G(3,\ 7)u_3 + G(3,\ 8)u_{3,\ 11} \\ &+ G(3,\ 9)u_{3,\ 1111} + G(3,\ 10)u_{3,\ 1122} + G(3,\ 11)u_{3,\ 22} \\ &+ G(3,\ 12)u_{3,\ 2222} + G(3,\ 13)\phi_{1,\ 1} + G(3,\ 14)\phi_{1,\ 111} \\ &+ G(3,\ 15)\phi_{1,\ 122} + G(3,\ 16)\phi_{2,\ 112} + G(3,\ 17)\phi_{2,\ 2} \\ &+ G(3,\ 18)\phi_{2,\ 222} = -q \end{aligned} \tag{6}$$

where the constants $G(3, j)$, with $j = 1, \ldots, 18$, are as given by Eq. (A1) in the Appendix, and A_{ij}, B_{ij} etc., denote integrated laminate stiffness. The remaining four equilibrium equations are not presented here in the interest of brevity. The SS2 type simply supported boundary condition is given as follows:

$$u_1(0, x_2) = u_1(a, x_2) = u_2(x_1, 0) = u_2(x_1, a) = 0 \tag{7a}$$

$$u_3(0, x_2) = u_3(a, x_2) = u_3(x_1, 0) = u_3(x_1, a) = 0 \tag{7b}$$

$$\phi_1(x_1, 0) = \phi_1(x_1, b) = \phi_2(0, x_2) = \phi_2(a, x_2) = 0 \tag{7c}$$

$$N_6(0, x_2) = N_6(a, x_2) = N_6(x_1, 0) = N_6(x_1, b) = 0 \tag{7d}$$

$$M_1(0, x_2) = M_1(a, x_2) = M_2(x_1, 0) = M_2(x_1, b) = 0 \tag{7e}$$

$$P_1(0, x_2) = P_1(a, x_2) = P_2(x_1, 0) = P_2(x_1, b) = 0 \tag{7f}$$

The SS3 type simply supported boundary condition can be obtained by replacing Eqs. (7a) and (7d) by the following, keeping the rest of Eqs. (7) unaltered:

$$N_1(0, x_2) = N_1(a, x_2) = N_2(x_1, 0) = N_2(x_1, b) = 0 \tag{8a}$$

$$u_2(0, x_2) = u_2(a, x_2) = u_1(x_1, 0) = u_1(x_1, b) = 0 \tag{8d}$$

Solution Methodology

The present solution strategy is based on a recently developed double Fourier series approach[24] for solution of a system of highly coupled PDEs with constant coefficients, subjected to arbitrary admissible boundary conditions. This method facilitates the well-posed quality of the Fourier formulation through selection of the coefficients of the assumed double Fourier series solutions for the unknown functions and the introduction of certain boundary Fourier coefficients, so that the number of equations become equal to the number of unknown coefficients to furnish a complete solution. Presence of discontinuities of the assumed solution functions or their first derivatives at the boundaries, which yield additional unknown coefficients, is handled by utilizing a mathematical approach based on Lebesgue measure theory (see, e.g., Chaudhuri[24,25] and Carslaw[26]). The particular solution to the boundary-value problem of a cross-ply shell, given by Eqs. (6) and (7) is assumed as follows[24,25]:

$$u_1 = \sum_{m=0}^{\infty}\sum_{n=1}^{\infty} U_{mn}\cos(\alpha x_1)\sin(\beta x_2) \quad 0 < x_1 < a;\ 0 < x_2 < b \tag{9a}$$

$$u_2 = \sum_{m=1}^{\infty}\sum_{n=0}^{\infty} V_{mn}\sin(\alpha x_1)\cos(\beta x_2) \quad 0 < x_1 < a;\ 0 < x_2 < b \tag{9b}$$

$$u_3 = \sum_{m=1}^{\infty}\sum_{n=1}^{\infty} W_{mn}\sin(\alpha x_1)\sin(\beta x_2) \quad 0 \le x_1 \le a;\ 0 \le x_2 \le b \tag{9c}$$

$$\phi_1 = \sum_{m=0}^{\infty}\sum_{n=1}^{\infty} X_{mn}\cos(\alpha x_1)\sin(\beta x_2) \quad 0 \le x_1 \le a;\ 0 \le x_2 \le b \tag{9d}$$

$$\phi_2 = \sum_{m=1}^{\infty}\sum_{n=0}^{\infty} Y_{mn}\sin(\alpha x_1)\cos(\beta x_2) \quad 0 \le x_1 \le a;\ 0 \le x_2 \le b \tag{9e}$$

in which $\alpha = m\pi/a$ and $\beta = n\pi/b$. The total number of unknown constant coefficients introduced in Eqs. (9) is $5mn + 2m + 2n$. The next operation will be comprised of differentiation of the assumed solution functions, which is a necessary step before their substitution into the equilibrium equations (6). The procedure for differentiation of the assumed double Fourier series solution functions is based on Lebesgue (integration) theory that introduces boundary Fourier coefficients arising from discontinuities of the assumed solution functions.[24] It has recently been established that the boundary Fourier terms serve as the complementary solution to the boundary-value problem under consideration.[25] The procedure imposes certain constraints, the details of which are available in Chaudhuri[25] and, hence, are excluded here in the interest of brevity of presentation. The partial derivatives, which cannot be obtained by termwise differentiation, are given as follows[24,25]:

$$\begin{aligned} u_{1,2} &= \tfrac{1}{4}a_0 + \sum_{m=1}^{\infty}\frac{1}{2}a_m\cos(\alpha x_1) \\ &+ \frac{1}{2}\sum_{n=1}^{\infty}[\beta U_{0n} + \gamma_n a_0 + \psi_n b_0]\cos(\beta x_2) \\ &+ \sum_{m=1}^{\infty}\sum_{n=1}^{\infty}[\beta U_{mn} + \gamma_n a_m + \psi_n b_m]\cos(\alpha x_1)\cos(\beta x_2) \end{aligned}$$

$$\begin{aligned} u_{1,11} &= \sum_{m=1}^{\infty}\frac{1}{2}c_n\sin(\alpha x_1) \\ &+ \sum_{m=1}^{\infty}\sum_{n=1}^{\infty}\left[-\alpha^2 U_{mn} + \gamma_m c_n + \psi_m d_n\right]\cos(\alpha x_1)\sin(\beta x_2) \end{aligned}$$

$$\begin{aligned} u_{2,1} &= \tfrac{1}{4}e_0 + \frac{1}{2}\sum_{n=1}^{\infty}e_n\cos(\beta x_2) \\ &+ \frac{1}{2}\sum_{m=1}^{\infty}[\alpha V_{m0} + \gamma_m e_0 + \psi_m f_0]\cos(\alpha x_1) \\ &+ \sum_{m=1}^{\infty}\sum_{n=1}^{\infty}[\alpha V_{mn} + \gamma_m e_n + \psi_m f_n]\cos(\alpha x_1)\cos(\beta x_2) \end{aligned}$$

$$\begin{aligned} u_{2,22} &= \frac{1}{2}\sum_{m=1}^{\infty}g_m\sin(\alpha x_1) \\ &+ \sum_{m=1}^{\infty}\sum_{n=1}^{\infty}\left[-\beta^2 V_{mn} + \gamma_n g_m + \psi_n h_m\right]\sin(\alpha x_1)\cos(\beta x_2) \end{aligned}$$

$$\begin{aligned} u_{3,111} &= \frac{1}{2}\sum_{n=1}^{\infty}i_n\sin(\beta x_2) \\ &+ \sum_{m=1}^{\infty}\sum_{n=1}^{\infty}\left[-\alpha^3 W_{mn} + \gamma_m i_n + \psi_m j_n\right]\cos(\alpha x_1)\sin(\beta x_2) \end{aligned}$$

$$\begin{aligned} u_{3,222} &= \frac{1}{2}\sum_{m=1}^{\infty}k_m\sin(\alpha x_1) \\ &+ \sum_{m=1}^{\infty}\sum_{n=1}^{\infty}\left[-\beta^3 W_{mn} + \gamma_n k_m + \psi_n l_m\right]\sin(\alpha x_1)\cos(\beta x_2) \end{aligned}$$

$$\begin{aligned} \phi_{1,11} &= \frac{1}{2}\sum_{n=1}^{\infty}m_n\sin(\beta x_2) \\ &+ \sum_{m=1}^{\infty}\sum_{n=1}^{\infty}\left[-\alpha^2 X_{mn} + \gamma_m m_n + \psi_m n_n\right]\cos(\alpha x_1)\sin(\beta x_2) \end{aligned}$$

$$\begin{aligned} \phi_{2,22} &= \frac{1}{2}\sum_{m=1}^{\infty}o_m\sin(\alpha x_1) \\ &+ \sum_{m=1}^{\infty}\sum_{n=1}^{\infty}\left[-\beta^2 Y_{mn} + \gamma_n o_m + \psi_n p_m\right]\sin(\alpha x_1)\cos(\beta x_2) \end{aligned} \tag{10}$$

in which

$$(\gamma_i, \psi_i) = \begin{cases} (0, 1) & \text{if } i \text{ is odd} \\ (1, 0) & \text{if } i \text{ is even} \end{cases} \tag{11}$$

and where the constant coefficients a_m, b_m, etc. are as defined by Eq. (A2) in the Appendix. This step generates $8m+8n+4$ additional unknown Fourier coefficients, which represent the complementary solution. The remaining partial derivatives are obtained by termwise differentiation. Substitution of the assumed displacement functions and their appropriately obtained derivatives into the five governing PDEs yields $5mn + 2m + 2n$ linear algebraic equations. For example, Eq. (6) yields

$$\sum_{m=1}^{\infty}\sum_{n=1}^{\infty} \sin(\alpha x_1)\sin(\beta x_2)\big[\{-G(3,1)\alpha + G(3,2)\alpha^3 + G(3,3)\alpha\beta^2\}U_{mn} + \{-G(3,5)\beta + G(3,6)\beta^3 + G(3,4)\alpha^2\beta\}V_{mn} + \{G(3,7) - G(3,8)\alpha^2 + G(3,9)\alpha^4 + G(3,10)\alpha^2\beta^2 - G(3,11)\beta^2 - G(3,12)\beta^4\}W_{mn} + \{-G(3,13)\alpha + G(3,14)\alpha^3 + G(3,15)\alpha\beta^2\}X_{mn} + \{-G(3,17)\beta + G(3,18)\beta^3 + G(3,16)\alpha^2\beta\}Y_{mn} - G(3,2)\alpha(\gamma_m c_n + \psi_m d_n) + G(3,3)\alpha\beta(\gamma_n a_m + \psi_n b_m) - G(3,6)\beta(\gamma_n g_m + \psi_n h_m) + G(3,4)\alpha\beta(\gamma_m e_n + \psi_m f_n) - G(3,9)\alpha(\gamma_m i_n + \psi_m j_n) - G(3,12)\beta(\gamma_n k_m + \psi_n l_m) - G(3,14)\alpha(\gamma_m m_n + \psi_m n_n) - G(3,18)\beta(\gamma_n o_m + \psi_n p_m) - q_{mn}\big] = 0 \tag{12}$$

To match the number of unknown constant coefficients, the remaining groups of equations are supplied by the geometric and natural boundary conditions. It may be noted that the geometric boundary conditions (7b) and (7c) are automatically satisfied by the assumed solution functions (8c–8e). Satisfying the geometric boundary conditions (7a), e.g., vanishing of u_1 at the edges $x_1 = 0$, a, and equating the coefficients of $\sin(\alpha x_1)$, etc. yield the following linear algebraic equations:

$$\sum_{m=1}^{\infty} \psi_m U_{mn} = 0 \tag{13a}$$

$$U_{0n} + \sum_{m=1}^{\infty} \gamma_m U_{mn} = 0 \quad \text{for} \quad n = 1, 2, \ldots \tag{13b}$$

Similar equations result from vanishing of u_2 at the edges $x_2 = 0, b$. The last group of equations are obtained from satisfying the natural boundary conditions relating to N_6, M_1, M_2, P_1, and P_2, prescribed at the appropriate edges. For example, $N_6 = 0$ prescribed at the edges $x_1 = 0$ and a, yields

$$\sum_{n=1}^{\infty}\cos(\beta x_2)\left[\sum_{m=1}^{\infty}\bar{H}\beta U_{mn} + \tfrac{1}{2}\beta U_{0n} + \sum_{m=1}^{\infty}\bar{H}\alpha V_{mn} + \tfrac{1}{2}(\gamma_n a_0 + \psi_n b_0) + \sum_{m=1}^{\infty}(\gamma_n a_m + \psi_n b_m)\bar{H} + \tfrac{1}{2}e_n + \sum_{m=1}^{\infty}(\gamma_m e_n + \psi_m f_n)\right] = 0 \tag{14a}$$

$$\sum_{m=1}^{\infty}\bar{H}\{\alpha V_{m0} + \gamma_m e_0 + \psi_m f_0 + a_m) + \tfrac{1}{2}(a_0 + e_0) = 0 \tag{14b}$$

in which for the case of $N_6 = 0$ prescribed at the edges $x_1 = 0$ and a, $H = 1$ and $H = (-1)^m$, respectively. Similar equations result from satisfying $N_6 = 0$ prescribed at the edges $x_2 = 0$ and b; $M_1 = 0$ at the edges $x_1 = 0$ and a; $M_2 = 0$ at the edges $x_2 = 0$ and b; $P_1 = 0$ at the edges $x_1 = 0$ and a; and $P_2 = 0$ at the edges $x_2 = 0$ and b, which are omitted here in the interest of brevity of presentation.

On equating the coefficients of $\sin(\alpha x_1)\ \sin(\beta x_2)$, $\sin(\alpha x_1)$, etc. on both sides of Eqs. (12) and (14), the preceding operations result in $5mn + 10m + 10n + 4$ linear algebraic equations in total from Eqs. (12–14) in as many unknowns. In the interest of computational efficiency, the $5mn + 2m + 2n$ linear algebraic equations resulting from Eq. (12) and its counterparts (not shown here) are first solved for U_{mn}, V_{mn}, and W_{mn}, in terms of the boundary Fourier coefficients a_m, b_m, etc.[24] These are then substituted in the linear algebraic equations generated from the boundary conditions, i.e., Eqs. (13) and (14) and their counterparts, not shown here. This operation helps reduce the size of the problems under consideration by one or more orders of magnitude, depending on m, n, finally resulting in $8m + 8n + 4$ linear algebraic equations, which can be solved in a routine manner.

Numerical Results and Discussions

For illustrative purposes, numerical results for symmetric (0/90/0 deg) and antisymmetric (0/90 deg) cross-ply spherical panels of square planform, subjected to uniformly distributed transverse loads are presented. The following material properties are assumed.

Material type 1: $E_1 = 175.78$ GPa (25,000 ksi), $E_1/E_2 = 25$, $G_{12}/E_2 = G_{13}/E_2 = 0.5$, $G_{23}/E_2 = 0.2$, $\nu_{12} = 0.25$

Material type 2: $E_1 = 105.47$ GPa (15,000 ksi), $E_1/E_2 = 15$, $G_{12}/E_2 = G_{13}/E_2 = 0.4286$, $G_{23}/E_2 = 0.3429$, $\nu_{12} = 0.40$

Here E_1 and E_2 are the surface-parallel Young's moduli in x_1 and x_2 coordinate directions, respectively, and G_{12} denotes surface-parallel shear modulus. G_{13} and G_{23} are transverse shear moduli in the x_1–x_3 and x_2–x_3 planes, respectively, whereas ν_{12} is the major Poisson's ratio on the x_1–x_2 surface. The following normalized quantities are defined:

$$u_3^* = \frac{10^3 E_2 h^3}{q_0 a^4} u_3; \qquad M_1^* = \frac{10^3}{q_0 a^2} M_1$$

in which a is assumed equal to 812.8 mm (32 in.) and q_0 denotes the uniformly distributed transverse load. For all of the numerical results presented in Figs. 2–9 and Table 1, the displacement u_3 and moment M_1 are computed at the center of the panel.

Figure 2 displays the convergence (with $m = n$) of normalized transverse displacement (deflection) u_3^* and moment M_1^* of a moderately thick ($a/h = 10$) and moderately deep ($R/a = 10$) antisymmetric cross-ply (0/90 deg) spherical panel. Rapid and monotonic convergence is observed for u_3^*. Although the convergence plot of the central moment M_1^* exhibits an initially oscillatory convergence for $m = n \leq 20$, the oscillations die down very rapidly, rendering the convergence plot practically monotonic for $m, n \geq 5$ (Fig. 2). Figures 3 and 4 present comparisons of the central deflections u_3^*

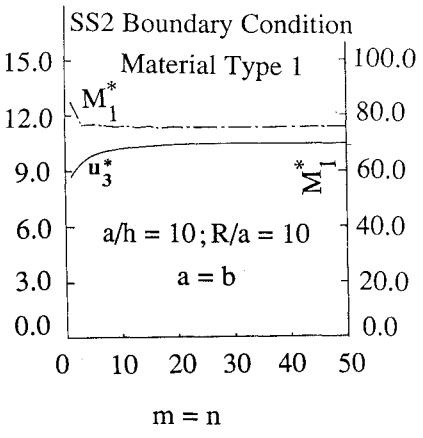

Fig. 2 Convergence of normalized central deflection and moment of a square moderately thick (a/h = 10) and moderately deep (R/a = 10) antisymmetric (0/90 deg) cross-ply spherical panel.

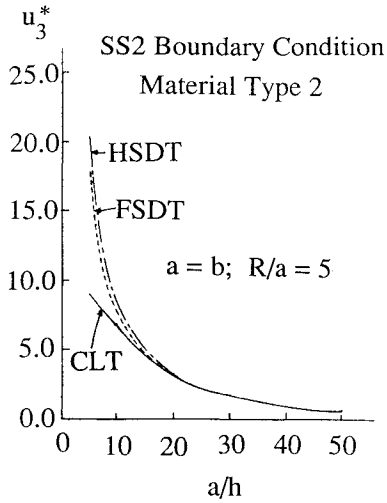

Fig. 3 Variation of normalized central deflection of a square relatively deep (R/a = 5) symmetric (0/90/0 deg) cross-ply spherical panel with a/h ratio and comparison with FSDT and CLT.

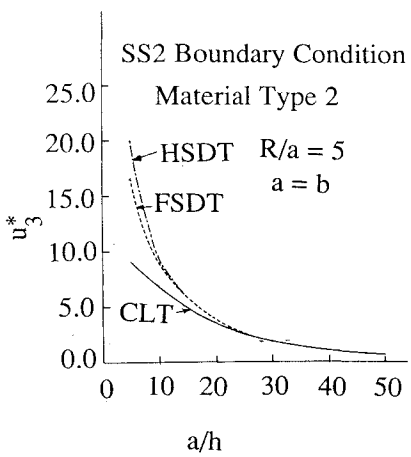

Fig. 4 Variation of normalized central deflection of a square relatively deep (R/a = 5) antisymmetric (0/90 deg) cross-ply spherical panel with a/h ratio and comparison with FSDT and CLT.

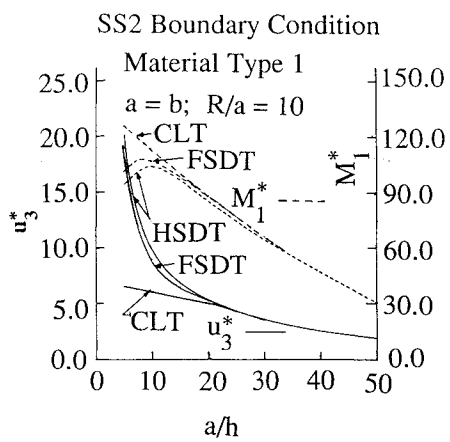

Fig. 5 Variation of normalized central deflection and moment of a square moderately deep (R/a = 10) symmetric (0/90/0 deg) cross-ply spherical panel with a/h ratio and comparison with FSDT and CLT.

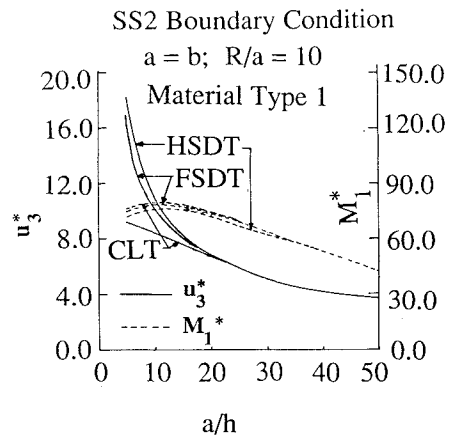

Fig. 6 Variation of normalized central deflection and moment of a square moderately deep (R/a = 10) antisymmetric (0/90 deg) cross-ply spherical panel with a/h ratio and comparison with FSDT and CLT.

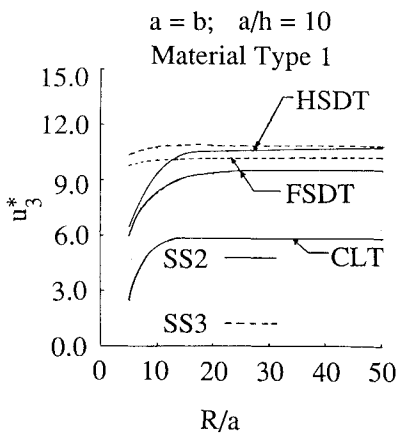

Fig. 7 Variation of normalized central deflection of square symmetric (0/90/0 deg) cross-ply spherical panels (a/h = 10) with R/a ratio for SS2 and SS3 boundary conditions.

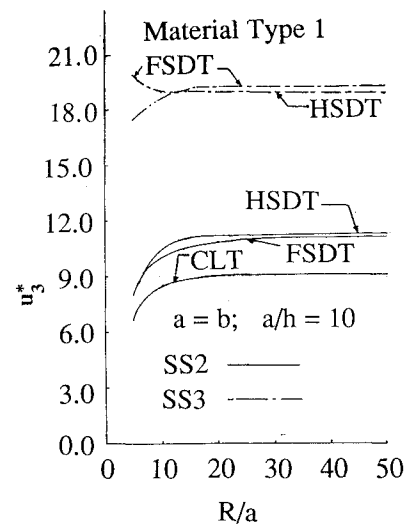

Fig. 8 Variation of normalized central deflection of square antisymmetric (0/90 deg) cross-ply spherical panels (a/h = 10) with R/a ratio for SS2 and SS3 boundary conditions.

Table 1 Percentages of error incurred by the CLT and FSDT based theories for square symmetric (0/90/0 deg) and antisymmetric (0/90 deg) cross-ply relatively deep ($R/a = 5$) spherical panels for various a/h ratios (material type 2)

Transverse displacement, u_3^*				
	Symmetric (0/90/0 deg)		Antisymmetric (0/90 deg)	
a/h	CLT, %	FSDT, %	CLT, %	FSDT, %
5.0	55.33	17.4	54.2	16.82
10.0	19.75	6.74	24.48	4.38
20.0	2. 44	1.4	6.1	0.51

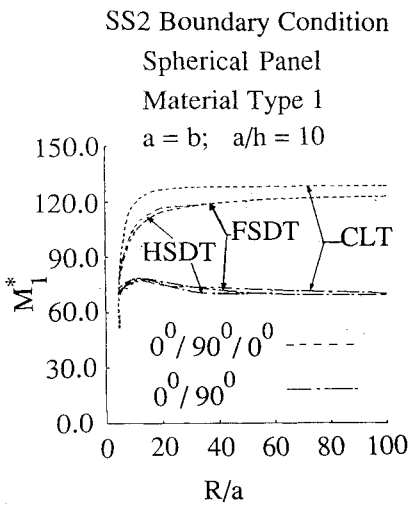

Fig. 9 Variation of normalized central moments of square symmetric (0/90/0 deg) and antisymmetric (0/90 deg) cross-ply spherical panels ($a/h = 10$) and with R/a ratio and comparison with FSDT and CLT.

of relatively deep ($R/a = 5$) symmetric (0/90/0 deg) and antisymmetric (0/90 deg) cross-ply panels, respectively, computed using the HSDT, FSDT, and CLT, with the material type 2, for various a/h ratios. Sensitivity of the response quantities of interest of thickness and lamination is self-evident in these plots. The shear correction factors, $K_1^2 = K_2^2 = 5/6$, are assumed in the present FSDT computations. Table 1 exhibits the percentages of error, defined by

$$\% \text{ Error} = 100\,[\text{HSDT} - \text{FSDT or CLT}]/\text{HSDT}$$

for lower a/h ratios. Accuracy of the HSDT in the thick panel regime ($a/h < 10$) is self-evident from Table 1 and Figs. 3 and 4, whereas the FSDT may be considered acceptable for moderately thick panels, $10 \leq a/h \leq 20$ and beyond. The CLT is best suited for relatively thin panels, $a/h \geq 20$. Figures 5 and 6 present variations, with respect to a/h ratio, of u_3^* and M_1^* of relatively shallow ($R/a = 10$) symmetric (0/90/0 deg) and antisymmetic (0/90 deg) cross-ply panels, respectively. It is interesting to observe from Figs. 5 and 6, that although the CLT and FSDT underpredict the computed normalized deflections in the thicker shell regime ($a/h \leq 20$), the reverse is true in the case of computed normalized moments. Furthermore, as expected[7,8] the thickness effect, especially in the case of thicker panels ($a/h \leq 20$), is more pronounced in the computed normalized deflections than in the corresponding moments. It is further noteworthy that a more pronounced thickness effect is observed in the computed central deflection and moment of symmetric (0/90/0 deg) panels, as compared to their antisymmetric (0/90 deg) counterparts. This view is also supported by Table 1, wherein the percentages of error incurred by the FSDT are shown to be somewhat reduced in the case of antisymmetric panels compared to their symmetric counterparts. There is reason to believe[27] that effect of thickness is compensated, to a certain extent, by the bending-stretching coupling effect, a characteristic of antisymmetric and unsymmetric laminates.

Variations of u_3^*, with respect to R/a ratio, of moderately thick ($a/h = 10$) symmetric (0/90/0 deg) and antisymmetric (0/90 deg) cross-ply panels, are presented in Figs. 7 and 8, respectively, for the SS2 and SS3 boundary conditions, whereas their M_1^* counterparts for the SS2 boundary condition are presented in Fig. 9. The SS3 plots in Figs. 7 and 8 are due to Reddy and Liu.[17] Sensitivity of the response quantities of interest to the curvature, lamination, and boundary constraint is self-evident in these plots. It is evident from Fig. 7 that the membrane action due to the curvature effect is very sensitive to the type of surface-parallel boundary constraint, i.e., $u_n = 0$ or $N_n = 0$ prescribed at an edge $x_n = \text{const}$. For example, variation of transverse displacements of symmetric (0/90/0 deg) cross-ply panels, with the SS3 boundary condition, is not that prominent, even in the deeper shell regime ($R/a < 10$) (Fig. 7). The same is not true, however, for the case of the SS2 boundary condition, where the membrane effect is quite pronounced, even for relatively shallow panels ($R/a \sim 10$). It is interesting to observe from Fig. 8 that in the case of antisymmetric (0/90 deg) cross-ply panels, the membrane action due to the effect of curvature has a complex interaction with the bending-streching type coupling effect, caused by the asymmetry of lamination. This interaction appears to be more pronounced in the case of prescribed simply supported boundary constraint, $u_n = 0$ (e.g., SS2 boundary condition), compared to that of simply supported boundary constraint $N_n = 0$ (e.g., SS3 boundary condition). Additionally, the bending-stretching type coupling has a highly pronounced interaction with the type of surface-parallel boundary constraint, far outweighing the effect of transverse shear deformation. For example, the normalized deflections of antisymmetric (0/90 deg) cross-ply panels in the case of prescribed simply supported boundary constraint $u_n = 0$, (i.e., SS2 boundary condition) are almost half of their counterparts for the case of prescribed simply supported boundary constraint $N_n = 0$ (i.e., SS3 boundary condition) (Fig. 8), whereas both types of boundary constraints yield comparable normalized deflection values for symmetric (0/90/0 deg) cross-ply panels (Fig. 7).

Summary and Conclusions

A heretofore unavailable analytical solution to the problem of deformation of a finite dimensional general cross-ply thick doubly curved panel of rectangular planform is presented. A solution methodology, based on a boundary-discontinuous generalized double Fourier series approach, which assures the wellposedness of the Fourier formulation and existence of the Fourier series solution, is used to solve a system of five highly coupled linear partial differential equations, with the SS2 type simply supported boundary condition. Unlike the conventional Navier and Levy type approaches which can only provide particular solutions, the present method is general enough to provide the complete (particular as well as the complementary) solution for any arbitrary combination of admissible boundary conditions with almost equal ease. The present paper is expected to serve as a reminder to future workers seeking a strong form of solutions to the laminated shell boundary-value problems that to derive the complementary solution and thus the complete solution they will have to look beyond the Navier and Levy methods. Numerical results presented here on cross-ply spherical panels demonstrate fast convergence, and comparisons with the available analytical solutions testify to the accuracy and efficiency of the method presented. The key conclusions that emerge from the numerical results can be summarized as follows.

1) Although no three-dimensional elasticity based strong form of solution that also meets the requirement of completeness is currently available in the literature, the trend appears to be that the CLT and the FSDT (with appropriate shear correction factor incorporated) underpredict the computed normalized deflections as compared to their HSDT counterparts in the thicker shell regime ($a/h \leq 20$), whereas the reverse is true in the case of computed normalized moments.

2) The effect of the transverse shear deformation is compensated to a certain extent by the bending-stretching coupling effect—a characteristic of unsymmetric laminates.

3) The membrane action due to the curvature effect is very sensitive to the type of surface-parallel boundary constraint, i.e., $u_n = 0$ or $N_n = 0$ prescribed at an edge $x_n = \text{const}$. Variation, with respect to R/a, of deflections, of symmetric (0/90/0 deg) cross-ply panels with the SS3 boundary condition is not that prominent, even in the deeper shell regime ($R/a < 10$). The same is not true, however, for the case of the SS2 boundary condition, where the membrane effect is quite pronounced, even for relatively shallow panels ($R/a \sim 10$).

4) Antisymmetric cross-ply spherical panels, by virtue of the bending-stretching coupling effect, are more sensitive to the type of surface-parallel boundary constraint, i.e., $u_n = 0$ or $N_n = 0$ prescribed at an edge $x_n = \text{const}$. The bending-stretching type coupling has a highly pronounced interaction with the type of surface-parallel boundary constraint, for outweighing the effect of transverse shear deformation. The normalized deflections of antisymmetric (0/90 deg) cross-ply panels in the case of prescribed simply supported boundary constraint $u_n = 0$ (i.e., SS2 boundary condition) are almost half of their counterparts for the case of prescribed simply-supported boundary constraint $N_n = 0$ (i.e., SS3 boundary condition), whereas both types of boundary constraints yield comparable normalized deflection values for symmetric (0/90/0 deg) cross-ply panels.

5) The membrane action due to the effect of curvature has a complex interaction with the bending-stretching type coupling effect, caused by the asymmetry of lamination. This interaction appears to be more pronounced in the case of prescribed simply supported boundary conditions with constraint $u_n = 0$ (e.g., SS2 boundary condition) compared to that of simply supported boundary constraint $N_n = 0$ (e.g., SS3 boundary condition).

Appendix: Definition of Certain Constants

The nonzero constants $G(3, j)$, $j = 1, \ldots, 18$, for an HSDT-based formulation, are

$$G(3,1) = -\frac{A_{11}}{R_1} - \frac{A_{12}}{R_2}; \qquad G(3,2) = \frac{4}{3h^2}E_{11}$$

$$G(3,3) = \frac{4}{3h^2}E_{12} + \frac{8}{3h^2}E_{66}$$

$$G(3,4) = \frac{4}{3h^2}E_{12} + \frac{8}{3h^2}E_{66}; \qquad G(3,5) = -\frac{A_{12}}{R_1} - \frac{A_{22}}{R_2}$$

$$G(3,6) = \frac{4}{3h^2}E_{22}$$

$$G(3,7) = -\frac{A_{11}}{R_1^2} - 2\frac{A_{12}}{R_1R_2} - \frac{A_{22}}{R_2^2};$$

$$G(3,8) = A_{55} - \frac{8}{h^2}D_{55} + \frac{16}{h^4}F_{55} + \frac{8}{3h^2}E_{11} + \frac{8}{3h^2}E_{12}$$

$$G(3,9) = -\frac{16}{9h^2}H_{11}; \qquad G(3,10) = -\frac{32}{9h^4}H_{12} - \frac{64}{9h^4}H_{66}$$

$$G(3,11) = A_{44} - \frac{8}{h^2}D_{44} + \frac{8}{3h^2R_1}E_{12} + \frac{8}{3h^2R_2}E_{22} + \frac{4}{h^2}D_{44}$$

$$G(3,12) = -\frac{16}{9h^4}H_{22}$$

$$G(3,13) = A_{55} - \frac{8}{h^2}D_{55} + \frac{F_{55}}{h^4} - \frac{B_{11}}{R_1} - \frac{B_{12}}{R_2} + \frac{4}{3h^2R_1}E_{11} + \frac{4}{3h^2R_2}E_{12}$$

$$G(3,14) = \frac{4}{3h^2}F_{11} - \frac{16}{9h^4}H_{11}$$

$$G(3,15) = \frac{4}{3h^2}F_{12} - \frac{16}{9h^4}H_{12} + \frac{8}{3h^2}F_{66} - \frac{32}{3h^4}H_{66}$$

$$G(3,16) = \frac{4}{3h^2}F_{12} + \frac{8}{3h^2}F_{66} - \frac{16}{9h^4}H_{12} - \frac{32}{9h^4}H_{66}$$

$$G(3,17) = A_{44} - \frac{8}{h^2}D_{44} + \frac{16}{h^4}F_{44} - \frac{B_{12}}{R_1} - \frac{B_{22}}{R_2} + \frac{4}{3h^2R_1}E_{12} + \frac{4}{3h^2R_2}E_{22}$$

$$G(3,18) = \frac{4}{3h^2}F_{22} - \frac{16}{9h^4}H_{22} \tag{A1}$$

The unknown Fourier coefficients, arising from edge discontinuities, are defined as

$$(a_m, b_m) = \frac{4}{ab}\int_0^a [\pm u_1(x_1, b) - u_1(x_1, 0)]\cos(\alpha x_1)\, dx \tag{A2a}$$

$$(c_n, d_n) = \frac{4}{ab}\int_0^b [\pm u_{1,1}(a, x_2) - u_{1,1}(0, x_2)]\sin(\beta x_2)\, dx_2 \tag{A2b}$$

in which the first term inside the parenthesis of the left side corresponds to the + sign. The boundary Fourier coefficient pairs—(g_m, h_m), (k_m, l_m), and (o_m, p_m)—can be obtained from Eq. (A2a) by replacing u_1 by $u_{2,2}$, $u_{3,22}$, and $\phi_{2,2}$, respectively. Likewise, the pairs—(e_n, f_n), (i_n, j_n), and (m_n, n_n)—can be obtained from Eq. (A2b) by replacing $u_{1,1}$ by u_2, $u_{3,11}$, and $\phi_{1,1}$, respectively.

References

[1]Mindlin, R. D., "Influence of Rotatory Inertia and Shear on Flexural Motions of Isotropic Elastic Plates," *Journal of Applied Mechanics*, Vol. 18, No. 1, 1951, pp. 31–38.

[2]Noor, A. K., and Burton, W. S., "Assessment of Shear Deformation Theories for Multilayered Composite Plates," *Applied Mechanics Reviews*, Vol. 42, No. 1, 1989, pp. 1–12.

[3]Noor, A. K., and Burton, W. S., "Assessment of Computational Models for Multilayered Composite Shells," *Applied Mechanics Reviews*, Vol. 43, No. 4, 1990, pp. 67–97.

[4]Pagano, N. J., "Exact Solution for Rectangular Bidirectional Composites and Sandwich Plates," *Journal of Composite Materials*, Vol. 4, Jan. 1970, pp. 931–933.

[5]Srinivas, S., and Rao, A. K., "Bending, Vibration and Buckling of Simply Supported Thick Orthotopic Rectangular Plates and Laminates," *International Journal of Solids and Structures*, Vol. 6, No. 11, 1970, pp. 1463–1481.

[6]Seide, P., "An Improved Approximate Theory for the Bending of Laminated Plates," *Mechanics Today*, edited by S. Nemat-Nasser, Pergamon, New York, Vol. 5, 1980, pp. 451–465.

[7]Chaudhuri, R. A., and Seide, P., "Triangular Finite Element for Analysis of Thick Laminated Plates," *International Journal for Numerical Methods in Engineering*, Vol. 24, No. 6, 1987, pp. 1563–1579.

[8]Seide. P., and Chaudhuri, R. A., "Triangular Finite Element for Analysis of Thick Laminated Shells," *International Journal for Numerical Methods in Engineering*, Vol. 24, No. 8, 1987, pp. 1563–1579.

[9]Chaudhuri, R. A., "An Equilibrium Method for Prediction of Transverse Shear Stresses in a Thick Laminated Plate," *Computers and Structures*, Vol. 23, No. 2, 1986, pp. 139–146.

[10]Chaudhuri, R. A., and Seide, P., "An Approximate Semi-Analytical Method for Prediction of Interlaminar Shear Stresses in an Arbitrarily Laminated Anisotropic Plate," *Computers and Structures*, Vol. 25, No. 4, 1987, pp. 627–636.

[11]Chaudhuri, R. A., and Seide, P., "An Approximate Method for Prediction of Transverse Shear Stresses in a Laminated Shell," *International Journal of Solids and Structures*, Vol. 23, No. 8, 1987, pp. 1145–1161.

[12]Chaudhuri, R. A., "A Semi-Analytical Approach for Prediction of Interlaminar Shear Stresses in Laminated General Shells," *International Journal of Solids and Structures*, Vol. 26, No. 4, 1990, pp. 499–510.

[13]Basset, A. B., "On the Extension and Flexure of Cylindrical and Spherical Thin Elastic Shells," *Philosophical Transactions of the Royal Society of London, Series A*, Vol. 181, No. 6, 1890, pp. 433–480.

[14]Nelson, R. B., and Lorch, D. R., "A Refined Theory for Laminated Orthotropic Plates," *Journal of Applied Mechanics*, Vol. 41, No. 1, 1974, pp. 177–183.

[15]Murthy, M. V. V., "An Improved Transverse Shear Deformation Theory for Laminated Anisotropic Plates," NASA Technical Paper 1903, 1981.

[16]Levinson, M., "An Accurate Simple Theory of the Statics and Dynamics of Elastic Plates," *Mechanics Research Communications*, Vol. 7, No. 6, 1980, pp. 343–350.

[17]Reddy, J. N., and Liu, C. F., "A Higher-Order Shear Deformation Theory of Laminated Elastic Shells," *International Journal of Engineering Science*, Vol. 23, No. 3, 1985, pp. 319–330.

[18]Librescu, L., Khdeir, A. A., and Frederick, D., "A Shear Deformable Theory of Laminated Composite Shallow Shell—Type Panels and Their Response Analysis I, Free Vibration and Buckling," *Acta Mechanica*, Vol. 76, Nos. 1–2, 1989, pp. 1–33.

[19]Chaudhuri, R. A., and Kabir, H. R. H., "Sensitivity of the Response of Moderately Thick Cross-Ply Doubly-Curved Panels to Lamination and Boundary Constraint—Part I: Theory; Part-II: Application," *International Journal of Solids and Structures*, Vol. 30, No. 2, 1992, pp. 263–272; 273–286.

[20]Hoff, N. J., and Rehfield, L. W., "Buckling of Axially Compressed Circular Cylindrical Shells at Stresses Smaller Than the Classical Critical Value," *Journal of Applied Mechanics*, Vol. 32, No. 3, 1965, pp. 542–546.

[21]Hughes, T. J. R., *The Finite Element Method*, Prentice-Hall, Englewood Cliffs, NJ, 1987.

[22]Seide, P., *Small Elastic Deformations of Thin Shells*, Ch. 1, Noordhoff International, Leyden, The Netherlands, 1975.

[23]Chaudhuri, R. A., "A Degenerate Triangular Shell Element with Constant Cross-Sectional Warping," *Computers and Structures*, Vol. 28, No. 3, 1988, pp. 315–325.

[24]Chaudhuri, R. A., "On Boundary-Discontinuous Double Fourier Series Solution to a System of Completely Coupled P.D.E.'s," *International Journal of Engineering Science*, Vol. 27, No. 9, 1989, pp. 1005–1022.

[25]Chaudhuri, R. A., "On Complete Boundary-Discontinuous Fourier Solution to a System of Completely Couple *n*th Order P.D.E.'s," Dept. of Civil Engineering, Univ. of Utah Rept., Salt Lake City, UT, June 1994.

[26]Carslaw, H. S., *Introduction to the Theory of Fourier's Series and Integrals*, 3rd ed., Dover, New York, 1930.

[27]Abu-Arja, K. R., and Chaudhuri, R. A., "Influence of Transverse Shear Deformation on Scaling of Cross-Ply Cylindrical Shells," *Journal of Composite Materials*, Vol. 23, July 1989, pp. 673–694.